Journal Homepage: -www.journalijar.com

INTERNATIONAL JOURNAL OF ADVANCED RESEARCH (IJAR)

Article DOI:10.21474/IJAR01/20006
DOI URL: http://dx.doi.org/10.21474/IJAR01/20006

RESEARCH ARTICLE

TWO NEWS HEPTAMOLYBDATES COMPOUNDS: SYNTHESIZES, ELECTROCHEMICAL PROPERTIES AND THERMAL STABILITY

Aboubacar Soumano[1], Papa Aly Gueye[1], Lamine Yaffa[1], Dame Seye[1,2], Assane Touré[1], Balla Fall[1], Carine Duhayon[4], Cheikh Abdoul Khadir Diop[1], Róbert Gyepes[4] and Mamadou Sidibé[1]

1. Mineral and Analytical Chemistry Laboratory, Department of Chemistry, Faculty of Science and Technology, Cheikh Anta Diop University, Dakar, Senegal.
2. Department of Chemistry and Physical, UFR Science and Technology, Iba Der Thiam University, Thies, Senegal.
3. Laboratoire de Chimie de Coordination du CNRS, BP 44099, 205 route de Narbonne,31077 Toulouse Cedex 4, France.
4. Department of Inorganic Chemistry HIavova 2030 (Albertov 8) 128 43 Praha 2, Czech Republic.

Manuscript Info

Manuscript History
Received: 05 October 2024
Final Accepted: 07 November 2024
Published: December 2024

Key words:-
Heptamolybdate, Polyoxometalate, Hybrid, Hydrogen Bonds, Organic Counterions

Abstract

In this paper, two new compounds, $(C_6H_{20}N_3)_2[Mo_7O_{24}].3H_2O$ (1) and$(C_6H_{14}N)_6[Mo_7O_{24}].CH_4O.5.5H_2O$ (2), have been synthesized by a one pot process at the reflux condition. Both compounds were characterized by infrared and UV-visible spectroscopy techniques, as well as by X-ray diffraction. The compound (1) crystallizes in the monoclinic system with the space group $P2_1/n$ and the compound (2) crystallizes in the monoclinic system but with the space group $P2_1/c$. The structure consists of a non-protonated heptamolybdates polyanions, stabilized by organoammonium groups and water molecules. The cohesion of the three-dimensional structure is ensured by hydrogen bonds between the polyanions, the organoammonium groups, and the water molecules, thereby providing significant stability to the compound.

Introduction:-

Polyoxometalates (POMs) are nanoclusters composed of transition metals with high oxidation states.[1]They are an exceptional brand of coordination compounds with wide range and precise composition and architecture. POMs have been demonstrated to possess unique redox, catalytic, magnetic, optical and bioactive properties and exhibit potential in multidisciplinary materials.[2–9]

In particular, the isopolyoxometalates (IPOMs) exhibit excellent electrochemical properties.[10–15]The design of POMs functionalized with organic groups, via a controllable synthesis, leads to crystallized hybrid architectures gained much attention because the combination of organic and inorganic components which provide new multi-functional hybrid materials [16–18]

Amongisopolyoxometalates, there are organic-inorganic hybrid heptamolybdates with a general formula of $(C_xH_yN_z)_{6-t}[H_tMo_7O_{24}]$.

Corresponding Author:- Papa Aly Gueye
Address:- Université Cheikh Anta Diop de Dakar, Sénégal.

These compounds characterized by the assembling POMs with organoammonium cationsleads to crystallized hybrid architectures in which the organic-inorganic interface is established via hydrogen bonding networks, this synergy effect leads to unique properties.

In this paper, we will focus on structural description and electrochemical propertiestwo new organic-inorganic hybrid heptamolybdates$(C_6H_{20}N_3)_2[Mo_7O_{24}].3H_2O$ and$(C_6H_{14}N)_6[Mo_7O_{24}].CH_4O.5.5H_2O$.

Experimental section

Synthesis

Ammonium molybdate $(NH_4)_6[Mo_7O_{24}].4H_2O$ (99%), 3,3'-iminobispropylamine $C_6H_{17}N_3$ (98%), hydrochloric acid HCl (37%), methanol (99%) and cyclohexylamine $C_6H_{13}N$ (99%) were purchased from Sigma-Aldrich and used without further purification.

Both compounds were obtained using one pot synthesis process.

The compound $(C_6H_{20}N_3)_2[Mo_7O_{24}]\cdot 3H_2O$ (1) was obtained by mixing, in 40 mL of water, 5mmol (0,980 g) of ammonium molybdate and 5 mmol (0,676 g) of 3,3'-iminobispropylamine.

The compound $(C_6H_{14}N)_6[Mo_7O_{24}]\cdot CH_4O\cdot 5.5H_2O$ (2) was obtained by mixing 5 mmol (0,501 g) of ammonium molybdate and 5 mmol (0,676 g) of cyclohexylaminein 40 mL of solvent composed of 30 mL of water and 10 mL of methanol,

The pH of both solutions was adjusted to 6.5 with the addition of hydrochloric acid. The solutions were stirred for two hours and colorless crystals suitable for X-ray diffraction were obtained after slow evaporation.

X-ray diffraction

For compound (1), single-crystal X-ray diffraction data were collected with a Bruker-Nonius Kappa CCD diffractometer (MoKa radiation k = 0.71073 Å). The crystal to detector distance was 60 mm. Absorption corrections were considered using SADABS. [19]The determination was carried out using direct methods

For compound (2), single-crystal X-ray diffraction data were measured on a CrysAlis PRO (Rigaku Oxford Diffraction, 2021) diffractometer (CuKα radiation, λ = 1.54184Å). Data collection reduction and multi-scan ABSPACK correction were performed with CrysAlisPro (Rigaku Oxford Diffraction). The crystal including the anisotropic displacement parameters were refined with SHELXT-2013. [20–25]Crystallographic Information Files were compiled with Olex2.12or Crystals 15.4.1.Crystallographic data are summarized in table 1.

Table 1:- Crystal data and structure refinement for compounds (**1**) and (**2**).

Compounds	**(1)**	**(2)**
Molecular formula	$(C_6H_{20}N_3)_2[Mo_7O_{24}]\cdot 3H_2O$	$(C_6H_{14}N)_6[Mo_7O_{24}]\cdot CH_4O\cdot 5.5(H_2O)$
Formula weight (g.mol^{-1})	1378.13	1787.80
Crystal color, habit	Block, colorless	Block, colorless
Crystal system	Monoclinic	Monoclinic
a(Å)	8.8353 (3)	10.3263 (1)
b(Å)	20.6069 (5)	32.4556 (5)
c(Å)	19.2323 (6)	19.1711 (3)
α(deg)	90	90
β(deg)	91.9700 (10)	90.130 (1)
γ(deg)	90	90
V(Å^3)	3499.52 (18)	6425.11 (15)
Space group	$P2_1/n$	$P2_1/c$
Radiation type	MoKα	Cu Kα
Crystal size (mm)	0.350× 0.263 × 0.238	0.25 × 0.15 × 0.10
T_{min}, T_{max}	0.49/ 0.58	0.11/0.31
Z	4	4
F(000)	2680	3544
θ range, deg	2.1–28.3	2.7–71.9

Absorption coefficient, mm^{-1}	2.533	11.57
T(K)	120	100
λ(Å)	0.71073	1.54180
Reflections collected	58746	68079
Independent reflections	8687[R_{int} =0.355]	13709[R_{int} = 0.064]
Final R indices, I > 2□ (I)	R_1 = 0.0197, wR_2 = 0.0416	R_1 = 0.059, wR_2 = 0.134
GOF on F^2	1.093	1.019
Peak, hole/eÅ^{-3}	$\Delta\rho_{min}$ = –0.587, $\Delta\rho_{max}$ = 0.456	$\Delta\rho_{min}$ = –2.08, $\Delta\rho_{max}$ = 2.62

Spectroscopy

The UV-Visible absorption spectra were recorded using a Thermo Scientific GENESYS 10S UV-Vis spectrophotometer at room temperature in H_2SO_4 aqueous or distilled water solution. For all compounds, 15 mg was solubilized in 10 mL of sulfuric acid solution (2M) and distilled water for (1) and (2), respectively. A scan between 200 nm and 1100 nm was carried out for each compound. Sulfuric acid /distilled water was used as blank.

IR spectroscopy measurements were carried out for both compounds. IR measurements were performed using ATR (Attenuated Total Reflectance) method from 4000 to 400 cm^{-1}.[26]

Thermogravimetric measurements and Differential Scanning Calorimetry

Thermogravimetric (TG) and Differential Scanning Calorimetry (DSC) measurements were carried out with a SetaramSensysEvo under Argon flow, from room temperature to 800 °C, with a heating rate of 5 °C/min.

Electrochemical properties

Electrochemical measurements were carried out using a DropSensμStat-I 400 as a potentiostat/galvanostat instrument. They were performed using three electrodes cell consisting of a glassy carbon electrode (0.07cm^2 surface area) as the working electrode, a reference electrode (Ag/AgCl, 1M KClsatured) and a platinum wire as the counter electrode.

The electrochemical proprieties of compounds (1) and (2) were respectively investigated using 10 mL of aqueous acid medium (0.1 M H_2SO_4) and distilled water, with a scan rate of 25 mV/s.

The electrochemical measurements with different scanning rates from 10 mV/s to 45 mV/s were also performed in the same conditions.

Results and Discussion:-

Structure description of (1) and (2)

Compound**(1)** crystallizes in monoclinic system with the space group $P2_1/n$ and the asymmetric unitconsists of one heptamolybdate anion, two 3,3'-iminobispropylammonium cations and three water molecules (Figure 1.a). Whereas the compound **(2)** crystallizes in monoclinic system with the space group $P2_1/c$ and the asymmetric unitis composed of oneheptamolybdate polyanion, sixcyclohexylammonium cations, one molecule of methanol and five water molecules (Figure1.b). The polyhedral description of the heptamolybdate polyanion $[Mo_7O_{24}]^{6-}$consists ofsix octahedra (MoO_6) linked together by edge sharing. These six octahedra (MoO_6)forms crown around a central Mo(VI) in an octahedral environment.

Bond-valence sum calculations yield average for all Mo atoms to +6 and all O atoms are in the -2-oxidation state. We can distinguish four categories ofMo─O bonds in each polyanion: (a) Mo─O_t, (O_t = terminal oxygen) with bond lengths range of1.707(2)─1.737(2) Å for compound (1), and 1.701(5)─1.729(5) Å for compound (2); (b) Mo─(μ_1-O) (μ_1-O= oxygen atoms bridging two molybdenum atoms) with bond lengths range of 1.735(2)─2.543(2) Å for compound (1), and1.737(5)─2.522(5) Å for compound (2); (c) Mo─(μ_2-O), (μ_2-O = oxygen atoms bridging three molybdenum atoms), with bond lengths between 1.894(2) to 2.287(2) Å for compound (1), and 1.883(4) to 2.283(5) Å for compound (2); (d) Mo─(μ_3-O), ((μ_3-O) = oxygen atoms bridging four molybdenum atoms) with bond lengths range of 2.135(2)─2.259(2) Å for compound (1), and 2.140(4)─2.294(4) Å for compound (2). All molybdenum atoms are linked to two terminal oxygen atoms except Mo_4, which is located in the center of the polyanion (Figure. 2.b).[27–31]

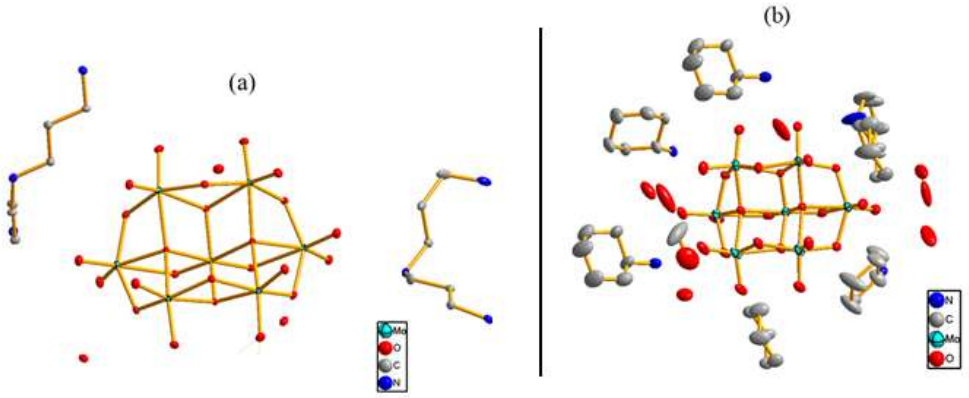

Figure 1:- Asymmetric units of (a) compound 1 and (b) compound 2.

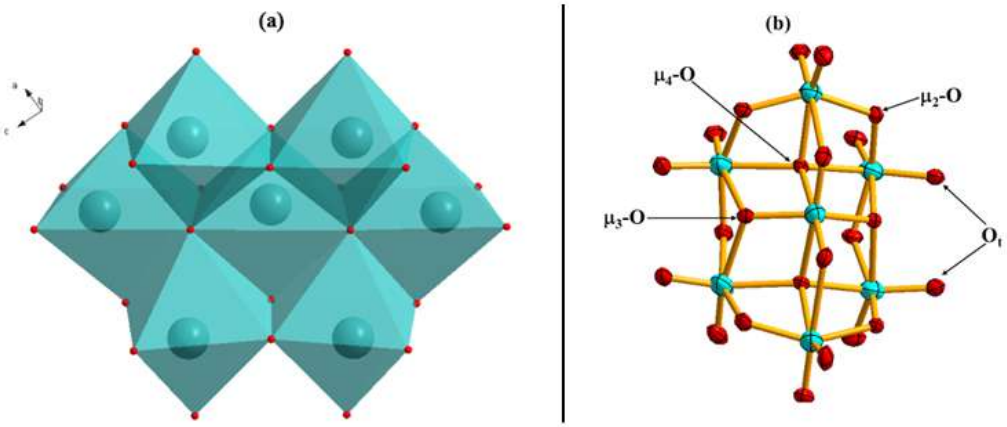

Figure 2:- Structures of the heptapolybdate polyanion. (a): polyhedral representation and (b): sticks representation with different types oxygen atoms.

Incompound (1), polyanions,organoammoniums cations and water molecules interact with each other viastrong hydrogen bonds networks: Ow—H···O, N—H···Ow, and N—H···O.

Water molecules act as hydrogen donors and hydrogen acceptors and have two types of hydrogen bonds. H_2O (O00N) molecule combine with $[Mo_7O_{24}]^{6-}$ anions through O_W—H···O bonds and with organic counterions through N—H···Owinteractions. Meanwhile, the second organic cation forms a H-bond with heptamolybdatevia N—H···O interactions. The N—H···O interaction between the $[Mo_7O_{24}]^{6-}$ anion and the $C_6H_{20}N_3^+$ cation results in the formation of a one-dimensional chain along the a-axis. This one-dimensional chain is connected by hydrogen bonds between cations, water molecules, and heptamolybdate units, forming a 3D network of alternating H_2O, $C_6H_{20}N_3^{3+}$ and $[Mo_7O_{24}]^{6-}$ molecules (Figure.3).Similar compounds have been published in several papers.

Table 2:- Selected hydrogen-bonding parameters (Å) for compounds 1 and 2.

$(C_6H_{20}N_3)_2[Mo_7O_{24}].3H_2O(1)$				**$(C_6H_{14}N)_6[Mo_7O_{24}].CH_4O.5.5H_2O$ (2)**			
D─H···A	d(D─H)	d(H···A)	d(D···A)	D─H···A	d(D─H)	d(H···A)	d(D···A)
N8─H14···O00V	0.918	1.995	2.812	**C9—H91···O7i**	**1.00**	**2.47**	**3.095 (15)**
N10─H41···O00B	0.76	2.079	2.806	**C28—H282···O37i**	**0.97**	**2.50**	**3.433 (15)**
C01C─H177···O00O	0.979	2.565	3.428	**C37—H371···O2**	**0.98**	**2.53**	**3.258 (15)**
C01D─H29···O00Q	0.98	2.485	3.141	**C37—H371···O17**	**0.98**	**2.53**	**3.207 (15)**
O00N─H59···O00R	0.758	2.028	2.785	**N29—H291···O35**	**0.90**	**1.97**	**2.864 (15)**
N9─H24···O00O	0.883	2.03	2.862	**N1—H11···O31**	**0.88**	**2.02**	**2.891 (15)**
				N36—H363···O21	**0.89**	**1.91**	**2.718 (15)**
				N8—H83···O23	**0.89**	**2.34**	**3.173 (15)**

				N29—H292···O19	**0.89**	**1.95**	**2.829 (7)**
				N29—H293···O13ii	**0.90**	**2.16**	**2.915 (7)**
				N8—H82···O1i	**0.89**	**1.95**	**2.788 (15)**
				N1—H12···O9	**0.89**	**1.97**	**2.836 (7)**
				N1—H13···O10iv	**0.88**	**2.57**	**3.143 (7)**
				N1—H13···O12iv	**0.88**	**2.02**	**2.876 (7)**
				N36—H361···O5	**0.89**	**1.86**	**2.719 (15)**
				N15—H152···O18	**0.89**	**2.31**	**2.995 (15)**
				N15—H152···O22	**0.89**	**2.06**	**2.766 (15)**
				N15—H153···O2i	**0.89**	**2.13**	**3.016 (15)**
				N15—H151···O11i	**0.89**	**2.18**	**2.804 (15)**
				N15—H151···O36ii	**0.89**	**2.24**	**2.968 (15)**
				N22—H222···O3i	**0.89**	**2.14**	**2.781 (15)**
				N22—H221···O1i	**0.90**	**2.31**	**3.097 (15)**

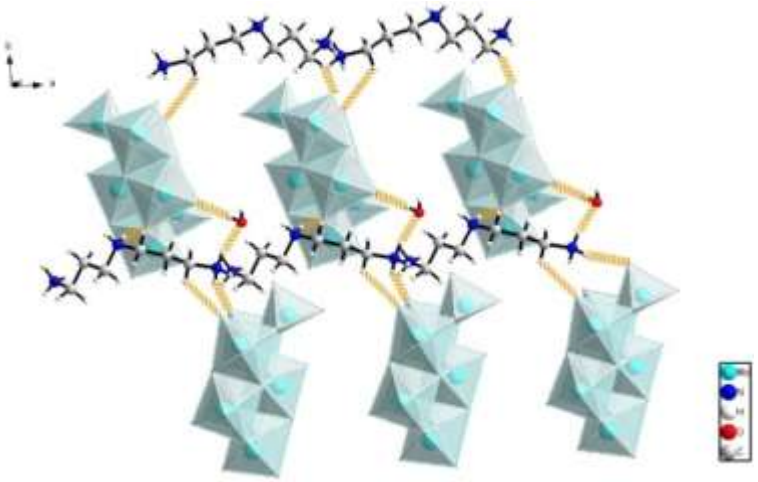

Figure 3:- Three-dimensional representation of compound (1).

In compound 2, the constituents are involved in two varieties of hydrogen bonds namely, O─H···O and N─H···O. The $[Mo_7O_{24}]^{6-}$ ions are bonded to organic cations through N─H···O hydrogen interactions leading the formation of a one-dimensional chain along the a-axis, on which $C_6H_{14}N^+$ and $[Mo_7O_{24}]^{6-}$molecules alternate (Figure 4).Watermolecules O32 and O33 bind togetherthroughhydrogenbondstoformfour-memberedringoligomers.Thelatterareplacedbetweenthechainsandensurethe formation of a three-dimensional structure.Similarcompounds in which watermoleculesformoligomersviahydrogenbondshavebeenreportedintheliterature.[32–35]

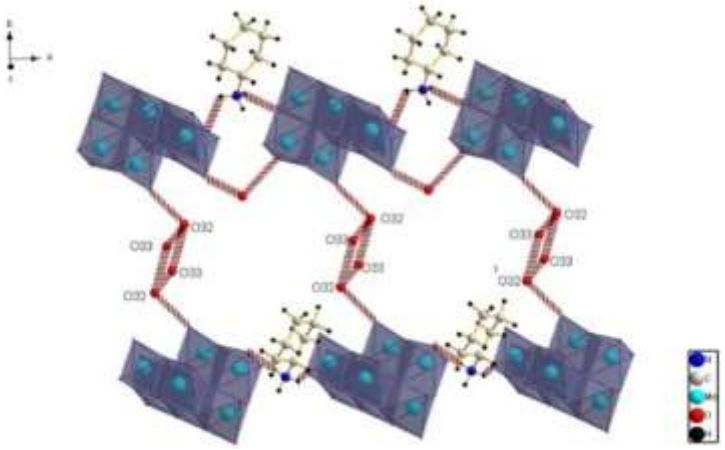

Figure 4:- Three-dimensional representation of compound (2).

Spectroscopy

The UV–Visible absorption of both compounds was analyzed in the range of 250–700 nm in acidic solution. In this region, only one single strongabsorption band is observed for both compounds. The UV spectra reveal precisely absorptions peaks at λmax equal 314 nm and 303 nm for compounds (1) and (2), respectively. This absorption band is attributed to Ligand-Metal Charge Transfer (LMCT) transition of the O→Mo(Figure 5). Indeed, during irradiation, electrons are promoted from low-energy electronic states, mainly composed of 2p oxygen orbitals, to the high-energy electron states, mainly made up of 4d metal orbitals of molybdenum. Then, both compounds absorb in the ultraviolet region.

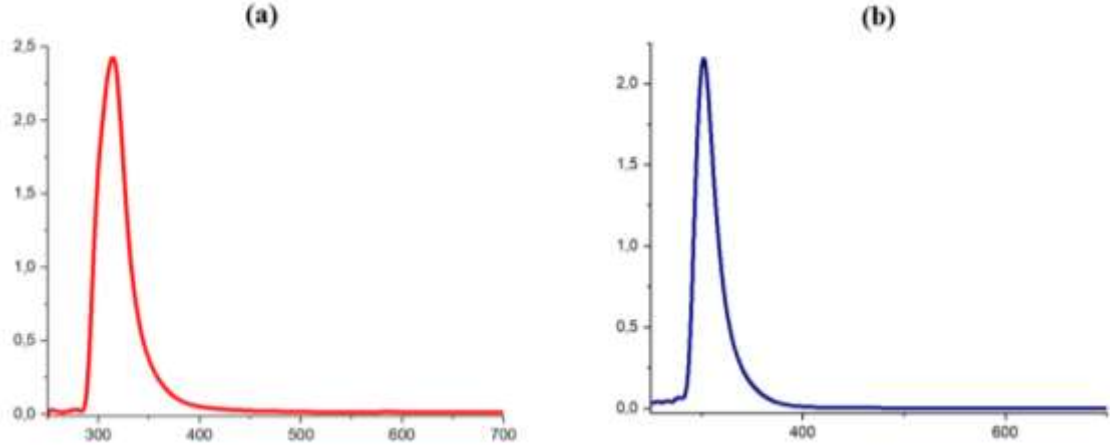

Figure 5:- Uv visible spectra:(a) for compound 1and (b) for compound 2.

In the IR spectrum of compound 1 (Figure 6), the characteristic bands at 926, 908, 831, and 615 cm^{-1} are attributed to (Mo—O) and (Mo—(-O)) vibrations bands based on the polyanion $[Mo_7O_{24}]^{6-}$ and the characteristic bands centeredat 1605, 1588, 1500, 1475, 1403, 1313, and 1261 cm^{-1} can be regarded as features symmetric/asymmetric absorption bands (N—H), (C—H) of the3,3'iminobispropylammonium cations.

The absorption band at 2988 cm^{-1} corresponds to ν(O–H) of water. In the IR spectrum of compound 2 (Figure. 4.SI), the characteristic bands at 922, 845, 610, and 558 cm^{-1} are attributed to (Mo—Ot) and (Mo—(-O)) vibrations bands based on the heptamolybdate polyanion $[Mo_7O_{24}]^{6-}$structure and characteristic bands centered at2969, 2768, 1417 to 1268 cm^{-1} can be regarded as features symmetric/asymmetric absorption bands (N—H), (C—H) of the cyclohexylammonium and methylamine.The O–H stretching bands of thewater of crystallization are observed at 3360 cm^{-1}.[36]

TG and DSC analysis

The thermal behaviours of the compounds were investigated by TGA–DSC analyses. The TGA and DSC curves for the obtained polyoxometalates have been shown in Figure 7.

The TGA curve of the prepared **compound 1**(Figure 7a) show a weight loss of 3.5% (calculated3.92%) in the range of130–200 °C. The corresponding DSC curve indicated an endothermic effect in this region.This weight loss could be assigned to the loss of tree water molecules. The next second weight loss of 19.7% (calculated 19.48%) between 200–400°C. In this range, the DSC cure show an exothermic peak. This weight loss is attributed to the degradation of the organic species, i.e. 3,3'-iminobispropylammonium groups in the hybrid material. The third weight loss is observed over 400°C with exothermic peaks showing in the DSC cure. This weight loss can be assigned to the decomposition of the polyanion in several steps according to the TGA curve and the DSC curve show several exothermic peaks. The total weight loss is 50%.

For the **compound 2**, the TGA curve(Figure 7b) showsthe first weight loss of 2% (calculated 1,79%) between 25–50°C. This weight loss is due to the elimination of methanol group. The second weight loss of 6% (calculated 5.54%) between 50–130°C. This weight loss is due to the elimination of water molecules. In this range the DSC curve show an endothermic peak. The third weight loss of 31 % (calculated 33.6%) observed in the range of 130–400°C can be attributed to the decomposition of six cyclohexylammonium groups. In this range, the DSC curve show an exothermic peak.

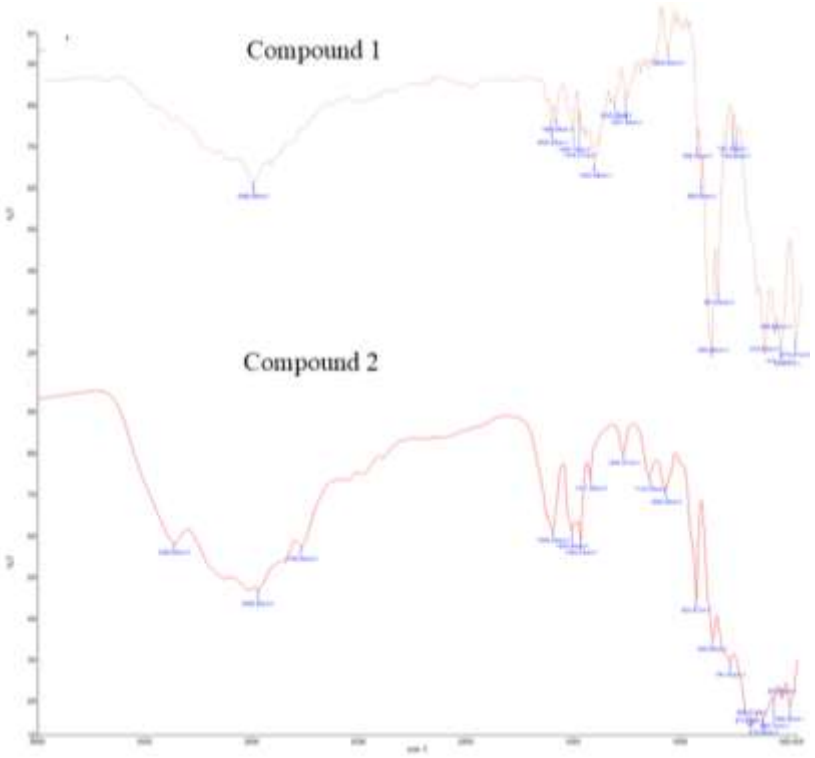

Figure 6:- IR spectra of compounds.

The last weight loss is observed over 400°C with exothermic peaks showing in the DSC cure. This weight loss can be assigned to the decomposition of the polyanion in several steps according to the TGA curve and the DSC curve show several exothermic peaks. The total weight loss is 30%.

The first degradation of compound 1 starts at 130 ^{o}C and for compound 2 the degradation starts at 25^{o}C,, showing the good stability of compound 1.[36–38]

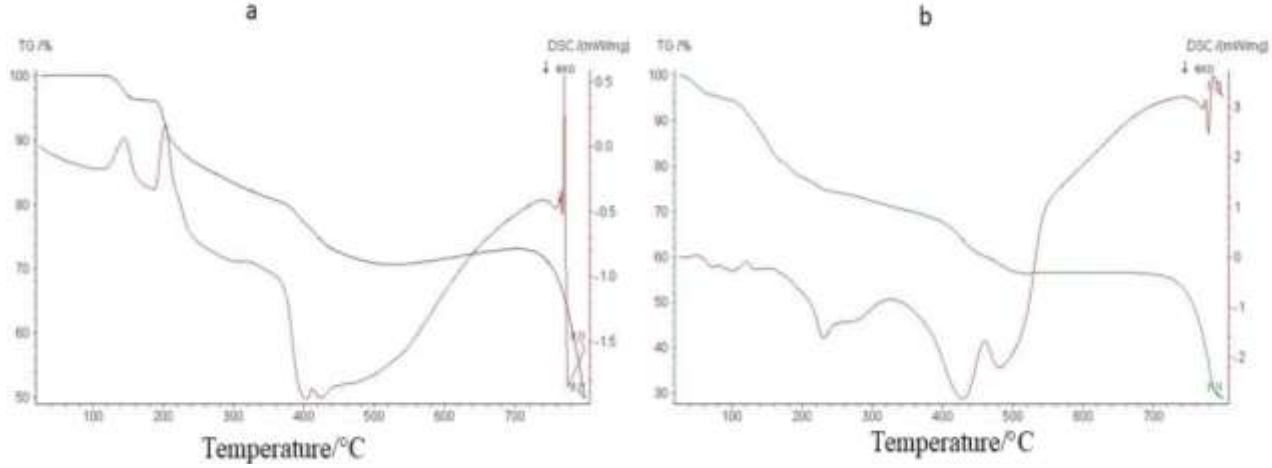

Figure 7:- TGA and DSC curves: (a) compound 1 and (b) compound 2.

Electrochemical properties

All electrochemical measurements were conducted using a μStat-i 400s MetrohmDropSenspotentiostat in a single-compartment three-electrode cell. The setup included a glassy carbon working electrode (4 mm diameter), a platinum wire counter electrode, and an Ag/AgCl reference electrode saturated with 3 M KCl. To investigate the electrochemical behavior of the compounds, cathodic scanning was performed within a potential range of -1500 to 1500 mV versus Ag/AgCl in 1 M H_2SO_4 aqueous solutions, at a scan rate of 30 mV/s. The recorded voltammograms

(see Figure 8) reveal two distinct anodic and cathodic peaks. The first redox process, with cathodic peak potentials (Epc) at approximately -0.055 V and -0.057 V for compounds 1 and 2 respectively (peak I), corresponds to the reduction from Mo(VI) to Mo(V). The second process, observed at Epc potentials of approximately 0.085 V and 0.083 V for compounds 1 and 2 respectively (peak II), indicates the reduction from Mo(V) to Mo(IV). [22,32] To further analyze the nature of the electrochemical processes, cyclic voltammograms (CVs) were recorded at various scan rates ranging from 5 to 100 mV/s within the same potential window. As illustrated in Figure 9, both anodic and cathodic peak currents increase with the scan rate. The linear relationship between peak currents and the square root of the scan rate suggests that the electrochemical reactions are diffusion-controlled processes.[39]

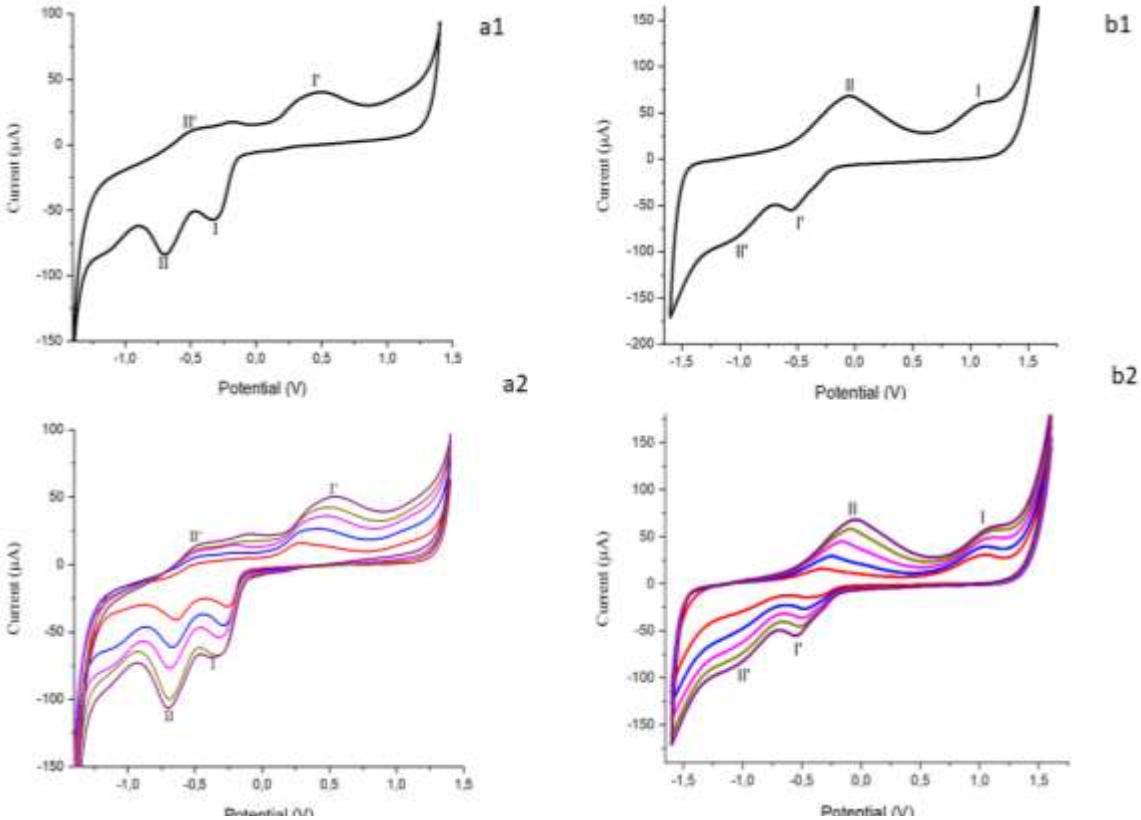

Figure 8:- Electrochemical measurements of compound (a1: Cyclic voltammograms with different scan rates, a2: Cyclic voltammograms at scan rate = 30 mV/s b1: Cyclic voltammograms with different scan rates, b2: Cyclic voltammograms at scan rate = 35 mV/s)

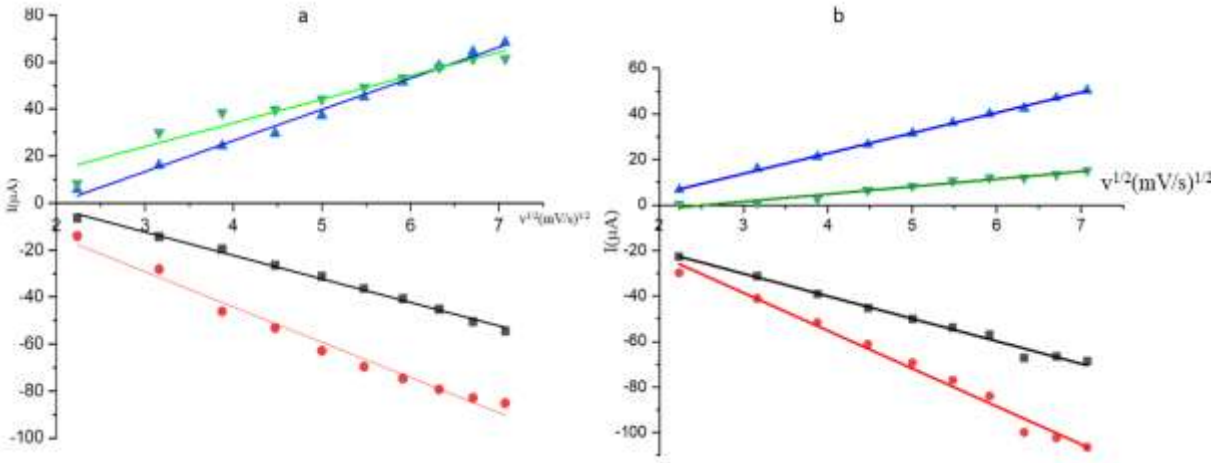

Figure 9:- Calibration curve for peak currents with respect to the square root of the scanning speed (a: compound 1 and b: compound 2).

Conclusion:-

In this work, we successfully synthesized two heptamolybdate-type POMs under a reflux condition which provides a new method of synthesized isopolyoxometalates as interacted with organoammonium groups and water molecules for constructing extended solid-state materials.

The structure of both compounds possesses a 3D supramolecular structure composed of amines, water and polyanion layers pillared chains. The present work may supply a potential method for forming other related pillared structures via alterations to POM building blocks.

The electrochemical properties of the title compounds were investigated and show for both compounds two reversible consecutive one-electron redox process and the square root of the scan rate indicates a diffusional process. These results show that for heptamolybdates, have a large number of hydrogen bonding interactions which contributes significantly to the thermal stability of the compounds. Therefore, this new thermally stable heptamolybdates could be an efficient catalyst for hydrogen peroxide oxygenation of organic sulfides.

Acknowledgments:-

The authors gratefully acknowledge the Cheikh Anta Diop University – Dakar (Senegal);

Departement of Inorganic Chemistry HIavova, Czech Republic and leLaboratoire de Chimie de Coordination du CNRS, Université de Toulouse, France.

References:-

(1) Liu, Q.; Wang, X. Polyoxometalate Clusters: Sub-Nanometer Building Blocks for Construction of Advanced Materials. Matter2020, 2 (4), 816–841.
(2) Pope, M. T.; Jeannin, Y.; Fournier, M. Heteropoly and Isopoly Oxometalates; Springer, 1983; Vol. 8.
(3) Pope, M. T.; Müller, A. Polyoxometalate Chemistry: An Old Field with New Dimensions in Several Disciplines. Angew. Chem. Int. Ed. Engl.1991, 30 (1), 34–48. https://doi.org/10.1002/anie.199100341.
(4) Ji, Y.; Huang, L.; Hu, J.; Streb, C.; Song, Y.-F. Polyoxometalate-Functionalized Nanocarbon Materials for Energy Conversion, Energy Storage and Sensor Systems. Energy Environ. Sci.2015, 8 (3), 776–789.
(5) Zhu, Y.; Huang, Y.; Li, Q.; Zang, D.; Gu, J.; Tang, Y.; Wei, Y. Polyoxometalate-Based Photoactive Hybrid: Uncover the First Crystal Structure of Covalently Linked Hexavanadate-Porphyrin Molecule. Inorg. Chem.2020, 59 (4), 2575–2583. https://doi.org/10.1021/acs.inorgchem.9b03540.
(6) Francese, R.; Civra, A.; Rittà, M.; Donalisio, M.; Argenziano, M.; Cavalli, R.; Mougharbel, A. S.; Kortz, U.; Lembo, D. Anti-Zika Virus Activity of Polyoxometalates. Antiviral Res.2019, 163, 29–33. https://doi.org/10.1016/j.antiviral.2019.01.005.
(7) Zang, D.; Huang, Y.; Li, Q.; Tang, Y.; Wei, Y. Cu Dendrites Induced by the Anderson-Type Polyoxometalate NiMo6O24 as a Promising Electrocatalyst for Enhanced Hydrogen Evolution. Appl. Catal. B Environ.2019, 249, 163–171. https://doi.org/10.1016/j.apcatb.2019.02.039.
(8) Zhang, Y.; Jiang, J.; Liu, Y.; Li, P.; Liu, Y.; Chen, L.; Zhao, J. Multi-Praseodymium-and-Tungsten Bridging Octameric Tellurotungstate and Its 2D Honeycomb Composite Film for Detecting Estrogen. Nanoscale2020, 12 (19), 10842–10853. https://doi.org/10.1039/D0NR01901A.
(9) Jiang, Z.-G.; Mao, W.-T.; Huang, D.-P.; Wang, Y.; Wang, X.-J.; Zhan, C.-H. A Nonconventional Host–Guest Cubic Assembly Based on γ-Cyclodextrin and a Keggin-Type Polyoxometalate. Nanoscale2020, 12 (18), 10166–10171. https://doi.org/10.1039/D0NR00973C.
(10) Rhule, J. T.; Hill, C. L.; Judd, D. A.; Schinazi, R. F. Polyoxometalates in Medicine. Chem. Rev.1998, 98 (1), 327–358.
(11) Hasenknopf, B. Polyoxometalates: Introduction to a Class of Inorganic Compounds and Their Biomedical Applications. Front Biosci2005, 10 (275), 10–2741.
(12) Aureliano, M.; Ohlin, C. A. Decavanadate in Vitro and in Vivo Effects: Facts and Opinions. J. Inorg. Biochem.2014, 137, 123–130. https://doi.org/10.1016/j.jinorgbio.2014.05.002.
(13) Aureliano, M.; Ohlin, C. A.; Vieira, M. O.; Marques, M. P. M.; Casey, W. H.; Batista De Carvalho, L. A. E. Characterization of Decavanadate and Decaniobate Solutions by Raman Spectroscopy. Dalton Trans.2016, 45 (17), 7391–7399. https://doi.org/10.1039/C5DT04176G.

(14) De Sousa, P. M. P.; Grazina, R.; Barbosa, A. D. S.; De Castro, B.; Moura, J. J. G.; Cunha-Silva, L.; Balula, S. S. Insights into the Electrochemical Behaviour of Composite Materials: Monovacant Polyoxometalates @ Porous Metal-Organic Framework. Electrochimica Acta2013, 87, 853–859. https://doi.org/10.1016/j.electacta.2012.09.099.
(15) Keita, B.; Nadjo, L.; Parsons, R. Surface Modifications with Heteropoly and Isopoly Oxometalates. J. Electroanal. Chem. Interfacial Electrochem.1989, 258 (1), 207–218. https://doi.org/10.1016/0022-0728(89)85173-3.
(16) Dolbecq, A.; Dumas, E.; Mayer, C. R.; Mialane, P. Hybrid Organic−Inorganic Polyoxometalate Compounds: From Structural Diversity to Applications. Chem. Rev.2010, 110 (10), 6009–6048. https://doi.org/10.1021/cr1000578.
(17) Proust, A.; Matt, B.; Villanneau, R.; Guillemot, G.; Gouzerh, P.; Izzet, G. Functionalization and Post-Functionalization: A Step towards Polyoxometalate-Based Materials. Chem. Soc. Rev.2012, 41 (22), 7605. https://doi.org/10.1039/c2cs35119f.
(18) Santoni, M.-P.; Hanan, G. S.; Hasenknopf, B. Covalent Multi-Component Systems of Polyoxometalates and Metal Complexes: Toward Multi-Functional Organic–Inorganic Hybrids in Molecular and Material Sciences. Coord. Chem. Rev.2014, 281, 64–85. https://doi.org/10.1016/j.ccr.2014.09.003.
(19) G.M. Sheldrick, SADABS, University of Göttingen, Germany, 2002.
(20) Otwinowski, Z.; Minor, W. [20] Processing of X-Ray Diffraction Data Collected in Oscillation Mode. In Methods in Enzymology; Macromolecular Crystallography Part A; Academic Press, 1997; Vol. 276, pp 307–326. https://doi.org/10.1016/S0076-6879(97)76066-X.
(21) Rigaku Oxford Diffraction (2021). CrysAlis PRO.
(22) Rigaku, (2021). XtaLAB Synergy-S.
(23) Watkin, D. J., Prout, C. K. & Pearce, L. J. (1996). CAMERON, Chemical Crystallography Laboratory, Oxford, UK.
(24) Betteridge, P. W.; Carruthers, J. R.; Cooper, R. I.; Prout, K.; Watkin, D. J. CRYSTALS Version 12: Software for Guided Crystal Structure Analysis. J. Appl. Crystallogr.2003, 36 (6), 1487–1487. https://doi.org/10.1107/S0021889803021800.
(25) Sheldrick, G. M. Crystal Structure Refinement with SHELXL. Acta Crystallogr. Sect. C Struct. Chem.2015, 71 (Pt 1), 3–8. https://doi.org/10.1107/S2053229614024218.
(26) FT-IR Spectroscopy-Attenuated Total Reflectance (ATR), Perkin Elmer Life and Analytical Sciences (2005).
(27) Li, T.; Lü, J.; Gao, S.; Cao, R. A New Heptamolybdate-Based Supramolecular Compound with an Alternating Organic and Inorganic Layer Structure: Synthesis, Crystal Structure and Properties of (Hapy)4[Co(H2O)5Mo7O24]•9H2O. Inorg. Chem. Commun.2007, 10 (11), 1342–1346. https://doi.org/10.1016/j.inoche.2007.07.018.
(28) Sci-Hub | | 10.11250/chimiothérapie1953.40.173. https://sci-hub.se/https://doi.org/10.11250/chemotherapy1953.40.173 (accessed 2024-02-10).
(29) Román, P.; San José, A.; Luque, A.; Gutiérrez-Zorrilla, J. M. Hexakis(Tert-Butylammonium) Heptamolybdate(VI)–Water (1/7). Acta Crystallogr. C1994, 50 (7), 1031–1034. https://doi.org/10.1107/S0108270193012831.
(30) Ftini, M. M. Characterization of an Inorganic-Organic Hybrid Polyoxomolybdate (C6H18N2)2[H2Mo7O24]•7H2O. J. Struct. Chem.2015, 56 (8), 1595–1601. https://doi.org/10.1134/S0022476615080211.
(31) Don, A.; Weakley, T. J. R. Guanidinium Heptamolybdate Monohydrate. Acta Crystallogr. B1981, 37 (2), 451–453. https://doi.org/10.1107/S0567740881003257.
(32) 晴久藤田; 知信藤田; 敏晴桜井; 淑子瀬戸. 新しい型の抗腫瘍物質, ポリオキソモリプデート. CHEMOTHERAPY1992, 40 (2), 173–178. https://doi.org/10.11250/chemotherapy1953.40.173.
(33) Wutkowski, A.; Srinivasan, B. R.; Naik, A. R.; Schütt, C.; Näther, C.; Bensch, W. Synthesis, Structure, and Photochemistry of an Organic Heptamolybdate-Monomolybdate. Eur. J. Inorg. Chem.2011, 2011 (14), 2254–2263. https://doi.org/10.1002/ejic.201001154.
(34) Pavani, K.; Ramanan, A. Influence of 2-Aminopyridine on the Formation of Molybdates under Hydrothermal Conditions. Eur. J. Inorg. Chem.2005, 2005 (15), 3080–3087. https://doi.org/10.1002/ejic.200500092.
(35) Roman, P.; Gutierrez-Zorrilla, J. M.; Martínez-Ripoll, M.; García-Blanco, S. Synthesis, Structure and Bonding of 2-Aminopyridinium Heptamolybdate Trihydrate. Transit. Met. Chem.1986, 11, 143–150. https://doi.org/10.1007/BF00637016.
(36) Sarr, B.; Mbaye, A.; Diallo, M. A.; Diop, C. A. K.; Sidibé, M.; Maury, F.; Charvillat, C.; Michaud, F. A New Good Thermal Stability Hybrid Material Based on Heptamolybdate Cluster: Synthesis and Structural Characterization. Chem. Data Collect.2020, 30, 100576.

(37) Qu, X.; Xu, L.; Yang, Y.; Li, F.; Guo, W.; Jia, L.; Liu, X. Hydrothermal Synthesis and Crystal Structure of Na(NH4)[C13N2H16]2[Mo7O24] • 8H2O: A Novel 3-D Extended Supramolecular Network with 1-D Channels. Struct. Chem.2008, 19 (5), 801–805. https://doi.org/10.1007/s11224-008-9367-y.
(38) Yaffa, L.; Kama, A. B.; Fall, B.; Traoré, B.; Diop, C. A.; Sidibé, M.; Diop, M.; Gautier, R. Synthesis, Crystal Structure and Electrochemical Properties of a New Methylammonium Sodium Decavanate Salt Na3 (CH3NH3) 3 [V10O28].(CH3NH2). 14H2O. J. Mol. Struct.2022, 1254, 132321.
(39) Yaffa, L.; Kama, A. B.; Sall, M. L.; Diop, C. A.; Sidibé, M.; Giorgi, M.; Diop, M.; Gautier, R. Role of the Organic Counterions on the Protonation of Strandberg-Type Phosphomolybdates. Polyhedron2020, 191, 114795.
(40) Wu, Y.; Zheng, J.; Xu, L.; Wang, Z.; Wen, D. Photo-Induced Electron Transfer and Electrocatalytic Properties of Novel Charge-Transfer Compound (TMB)3HPMo12O40. J. Electroanal. Chem.2006, 589 (2), 232–236. https://doi.org/10.1016/j.jelechem.2006.02.013.
(41) Dai, L.; Wang, E.; You, W.; Zhang, Z. Synthesis and Electrochemical Properties of a New 1D Organic–Inorganic Hybrid Compound Based on Keggin-Type Heteropolyanions and Isopolyanions Decorated by Transition Metal Fragments. J. Clust. Sci.2008, 19 (3), 511–519. https://doi.org/10.1007/s10876-008-0190-9.